Supporting Information

Alkaline-earth Metal Substitution Stabilizes Anionic Redox of Li-rich Oxides

Haoxin Li[ab], Xiaolin Zhao[ac], Yining Li[ac], Yang Gan[ac], Wujie Qiu*[ac], Jifen Wang*[b], and Jianjun Liu*[acd]

[a]State Key Laboratory of High Performance Ceramics and Superfine Microstructure, Shanghai Institute of Ceramics, Chinese Academy of Sciences, 1295 Dingxi Road, Shanghai 200050, China

[b]School of Science, College of Art and Science, Shanghai Polytechnic University, 2360 Jinhai Road, Shanghai 201209, China

[c]Center of Materials Science and Optoelectronics Engineering, University of Chinese Academy of Sciences, Beijing 100049, China

[d]School of Chemistry and Materials Science, Hangzhou Institute for Advanced Study, University of Chinese Academy of Science, 1 Sub-lane Xiangshan, Hangzhou, 310024, China

*Email: jliu@mail.sic.ac.cn; wjqiu1988@gmail.com; wangjifen@sspu.edu.cn

Calculation Details

The average voltage can be calculated from the free energy of the delithiation reaction:

$$V(x_1,x_2) = \frac{E(Li_{x1}Mg_{0.5}MnO_3) - E(Li_{x2}Mg_{0.5}MnO_3) - (x_1 - x_2)E(Li)}{(x_1 - x_2)F}$$

$(x_1 > x_2)$

where E($Li_{x1}Mg_{0.5}MnO_3$) and E($Li_{x2}Mg_{0.5}MnO_3$) are the DFT energies (T = 0 K). E(Li) is the DFT energy (T = 0 K) with bulk Li metal as the reference state. F is the Faraday constant. The oxygen vacancy formation energy can be used to determine the structural stability of O_2 loss in $Li_{1.5-x}Mg_{0.5}MnO_3$ during delithiation.

$$\Delta E_{vac} = E(Li_{1.5-x}Mg_{0.5}MnO_{3-\delta}) + \delta/2\mu(O_2) - E(Li_{1.5-x}Mg_{0.5}MnO_3)$$

where $E(Li_{1.5-x}Mg_{0.5}MnO_{3-\delta})$ represents the energy of $Li_{1.5-x}Mg_{0.5}MnO_3$ to remove the O atom (with the highest oxidation state was selected as the defect site), and $\mu(O_2)$ represent the chemical potential of oxygen at 300 K and 1 atm. The Crystal Orbital Hamilton Populations (COHP) analysis was performed using the Lobster program. The relative formation energy is used to evaluate the stability of $Li_{3-x}Mg_xTMO_4$ and $Li_3Mg_xTM_{1-x}O_4$ (TM=V, Nb):

$$\Delta H = \frac{E(Li_{3-x}Mg_xTMO_4) - (E(Li_3Mg_xTM_{1-x}O_4) + \frac{x}{2}E(TM_2O_5) - \frac{x}{2}E(Li_2O) - x\mu(O_2))}{n}$$

where $E(TM_2O_5)$ and $E(Li_2O)$ are the ground state of TM_2O_5 and Li_2O compounds, respectively. $E(Li_{3-x}Mg_xTMO_4)$ and $E(Li_3Mg_xTM_{1-x}O_4)$ are the total energy of the generated material, and $\mu(O_2)$ uses the chemical potential at temperature (300 K) and pressure (1 atm). Further, their free energy differences are computed through the

formula of $\Delta G_f=\Delta H_f-\Delta S*T$ (T=300K).

The average charge state of atoms at the same site is calculated through $\bar{v} = n_{valence} - \bar{n}_{mag}$, in which $n_{valence}$ and $\bar{n}_{mag}$ are valence electron number and average magnetic moment number of atoms at the same site.

Supplementary Tables

Table S1. Calculated energies (0K) and chemical potentials (300K) of the reference substances.

Compounds	Total Energy (eV/atom)
$E(Li_2CO_3)$	-6.19
$E(MnCO_3)$	-7.86
E(MgO)	-5.99
$\mu(CO_2)$	-7.74
$\mu(O_2)$	-5.16

Table S2. Total energies of Mg-substituting-Li compounds with the different substitution concentrations.

Mg concentration (%)	Mg-substituted-Li	Total Energy (eV/atom)
3.125	$Li_{31}Mg_1Mn_{16}O_{48}$	-18.58
6.250	$Li_{30}Mg_2Mn_{16}O_{48}$	-18.62
9.375	$Li_{29}Mg_3Mn_{16}O_{48}$	-18.66
12.500	$Li_{28}Mg_4Mn_{16}O_{48}$	-18.70
18.750	$Li_{26}Mg_6Mn_{16}O_{48}$	-18.77
25.000	$Li_{24}Mg_8Mn_{16}O_{48}$	-18.84
28.125	$Li_{23}Mg_9Mn_{16}O_{48}$	-18.89

Table S3. Total energies of Mg-substituting-Li and Li-vacancy compounds with the different substitution concentrations.

Mg concentration (%)	Mg-substituted-Li with Li vacancy	Total Energy (eV/ atom)
3.125	$Li_{30}Mg_1Mn_{16}O_{48}$	-18.43
6.250	$Li_{28}Mg_2Mn_{16}O_{48}$	-18.30
9.375	$Li_{26}Mg_3Mn_{16}O_{48}$	-18.18
12.500	$Li_{24}Mg_4Mn_{16}O_{48}$	-18.06
18.750	$Li_{20}Mg_6Mn_{16}O_{48}$	-17.82
25.000	$Li_{16}Mg_8Mn_{16}O_{48}$	-17.57
28.125	$Li_{14}Mg_9Mn_{16}O_{48}$	-17.46

Table S4. Total energies of Mg-substituting-Mn and Mn-vacancy compounds with the different substitution concentrations.

Mg concentration (%)	Mg-substituted-Mn	Total Energy (eV/atom)
6.250	$Li_{32}Mg_1Mn_{15}O_{48}$	-18.33
12.500	$Li_{32}Mg_2Mn_{14}O_{48}$	-18.11
18.750	$Li_{32}Mg_3Mn_{13}O_{48}$	-17.88
25.000	$Li_{32}Mg_4Mn_{12}O_{48}$	-17.66
37.500	$Li_{32}Mg_6Mn_{10}O_{48}$	-17.22
50.000	$Li_{32}Mg_8Mn_8O_{48}$	-16.78
56.250	$Li_{32}Mg_9Mn_7O_{48}$	-16.55

Table S5. Total energies of the 6 lowest energy structures of $Li_{1.5}Mg_{0.5}MnO_3$.

Configuration of $Li_{1.5}Mg_{0.5}MnO_3$	Total energy (eV/atom)	Relative energy(eV/atom)
S_1	-18.8647	0.0000
S_2	-18.8422	0.0225
S_3	-18.8272	0.0375
S_4	-18.7181	0.1466
S_5	-18.7050	0.1597
S_6	-18.6031	0.2616

Table S6. The total energy of the 6 lowest energy structures of $Li_{1.25}Mg_{0.5}MnO_3$.

Configuration of $Li_{1.25}Mg_{0.5}MnO_3$	Total energy (eV/atom)	Relative energy(eV/atom)
S_1	-18.2013	0.0000
S_2	-18.2009	0.0003
S_3	-18.1950	0.0063
S_4	-18.0806	0.1206
S_5	-17.9544	0.2469
S_6	-17.8625	0.3388

Table S7. The total energy of the 6 lowest energy structures of $Li_{1.0}Mg_{0.5}MnO_3$.

Configuration of $Li_{1.0}Mg_{0.5}MnO_3$	Total energy (eV/atom)	Relative energy(eV/atom)
S_1	-17.5766	0.0000
S_2	-17.5738	0.0028
S_3	-17.5734	0.0031
S_4	-17.5281	0.0484
S_5	-17.4953	0.0813
S_6	-17.4822	0.0944

Table S8. The total energy of the 6 lowest energy structures of $Li_{0.625}Mg_{0.5}MnO_3$.

Configuration of $Li_{0.625}Mg_{0.5}MnO_3$	Total energy (eV/atom)	Relative energy(eV/atom)
S_1	-16.4588	0.0000
S_2	-16.4434	0.0153
S_3	-16.4359	0.0228
S_4	-16.4216	0.0372
S_5	-16.3966	0.0622
S_6	-16.3956	0.0631

Table S9. The total energy of the 6 lowest energy structures of $Li_{0.375}Mg_{0.5}MnO_3$.

Configuration of $Li_{0.375}Mg_{0.5}MnO_3$	Total energy (eV/atom)	Relative total energy(eV/atom)
S_1	-15.6619	0.0000
S_2	-15.6491	0.0128
S_3	-15.6394	0.0225
S_4	-15.6331	0.0288
S_5	-15.5638	0.0981
S_6	-15.5472	0.1147

Table S10. The total energy of the 6 lowest energy structures of $Li_{0.25}Mg_{0.5}MnO_3$.

Configuration of $Li_{0.25}Mg_{0.5}MnO_3$	Total energy (eV/atom)	Relative total energy(eV/atom)
S_1	-15.2538	0.0000
S_2	-15.2534	0.0003
S_3	-15.2434	0.0103
S_4	-15.2403	0.0134
S_5	-15.2206	0.0331
S_6	-15.2175	0.0363

Table S11. The reversible capacity of Li_2MnO_3 and Mg-doped Li_2MnO_3 reported in the literature.

Compound	Reversible capacity (mAh/g)	Reference
Li_2MnO_3	120	*J. Electrochem. Soc.*, 2012, 159, A781
	128	*Electrochem. Commun.*, 2004, 6, 1085
	115	*Chem. Mater.*, 2015, 27, 3456
	115	This work
$Li_{1.98}Mg_{0.01}MnO_3$	260	*J. Power Sources*, 2016, 330, 37
	245	This work

Table S12. The bond length changes of different O-O bonding types during the delithiation process.

Type	O-O bond length (Å) (Mg-O-Li & Mg-O-Li)	O-O bond length (Å) (Li-O-Li & Mg-O-Li)	O-O bond length (Å) (Li-O-Li & Li-O-Li)
$Li_{1.5}Mg_{0.5}MnO_3$	2.880	2.631	2.718
$Li_{1.25}Mg_{0.5}MnO_3$	2.844	2.545	2.570
$Li_1Mg_{0.5}MnO_3$	2.791	2.505	1.445
$Li_{0.625}Mg_{0.5}MnO_3$	2.717	2.441	1.348
$Li_{0.375}Mg_{0.5}MnO_3$	2.741	2.422	1.323
$Li_{0.25}Mg_{0.5}MnO_3$	2.681	1.440	1.309

Table S13. Magnetic moment and valence state of atoms at same site in the three compounds.

Compound	Element	Average magnetic moment	Average valence state
MgO	Mg	0.00	+2.00
	O	0.00	-2.00
Li_2MnO_3	Mn	3.15	+3.85
	O	0.06	-1.94
$Li_{1.5}Mg_{0.5}MnO_3$	Mn1	3.20	+3.80
	Mn2	3.85	+3.15
	Mg	0.01	+1.99
	O	0.03	-1.97

Table S14. Relative formation energies were calculated for the substitution of the Li and TM sites by Mg in $Li_{2.125}Mg_{0.875}VO_4$ and $Li_{2.125}Mg_{0.875}NbO_4$.

Compounds	Relative formation energy (eV/atom)
V	-0.417
Nb	-0.401

Supplementary Figures

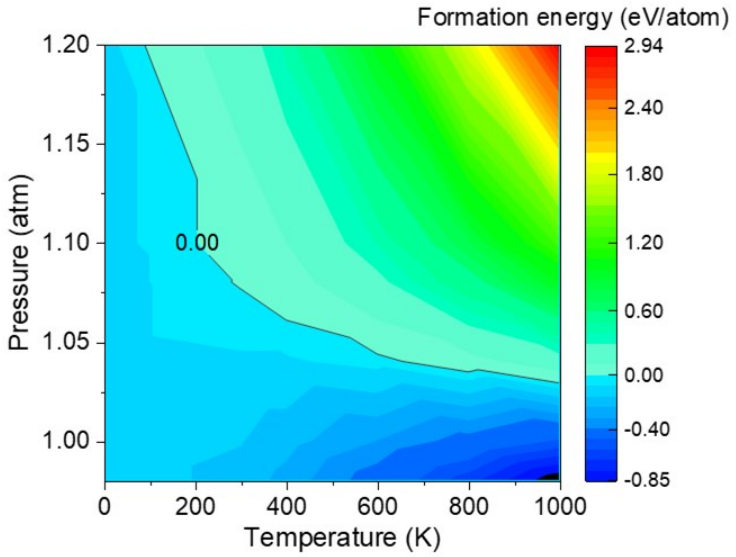

Figure S1. The formation energy of $Li_{1.5}Mg_{0.5}MnO_3$ as a function of temperature and pressure.

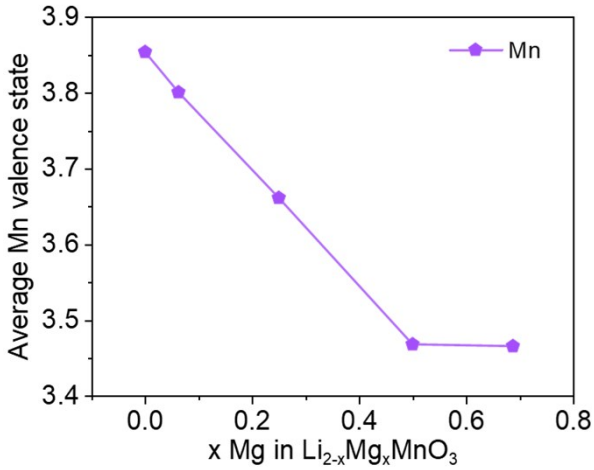

Figure S2. The change in the valence state of Mn ions in the state of increasing Mg proportion was obtained from the magnetic moment.

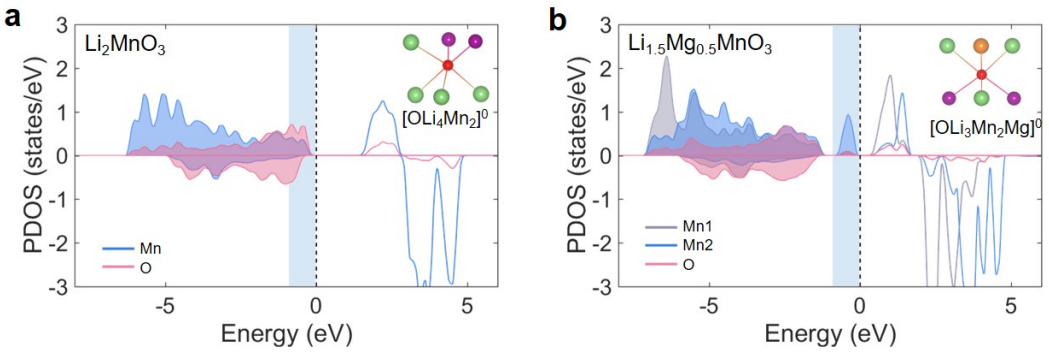

Figure S3. The pDOS of Mn and O in the O octahedra of Li_2MnO_3 (a) and $Li_{1.5}Mg_{0.5}MnO_3$ (b).

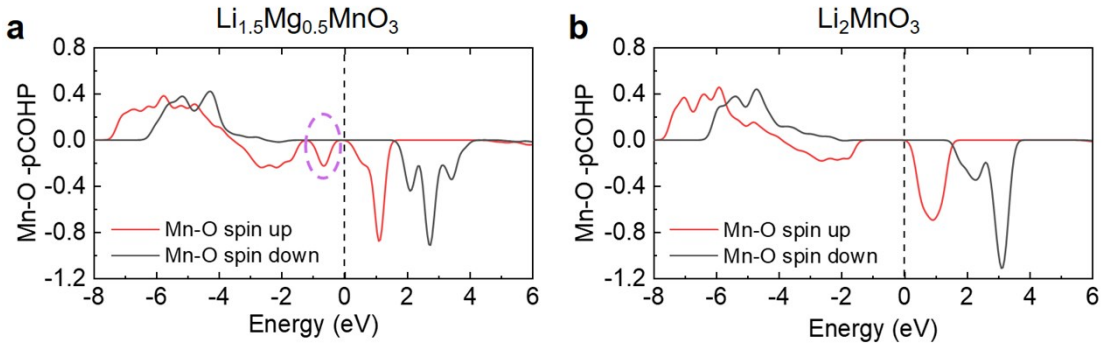

Figure S4. The pCOHP results for Mn-O bonds of $Li_{1.5}Mg_{0.5}MnO_3$ and Li_2MnO_3. Above zero is the bonding state and below zero is the anti-bonding state.

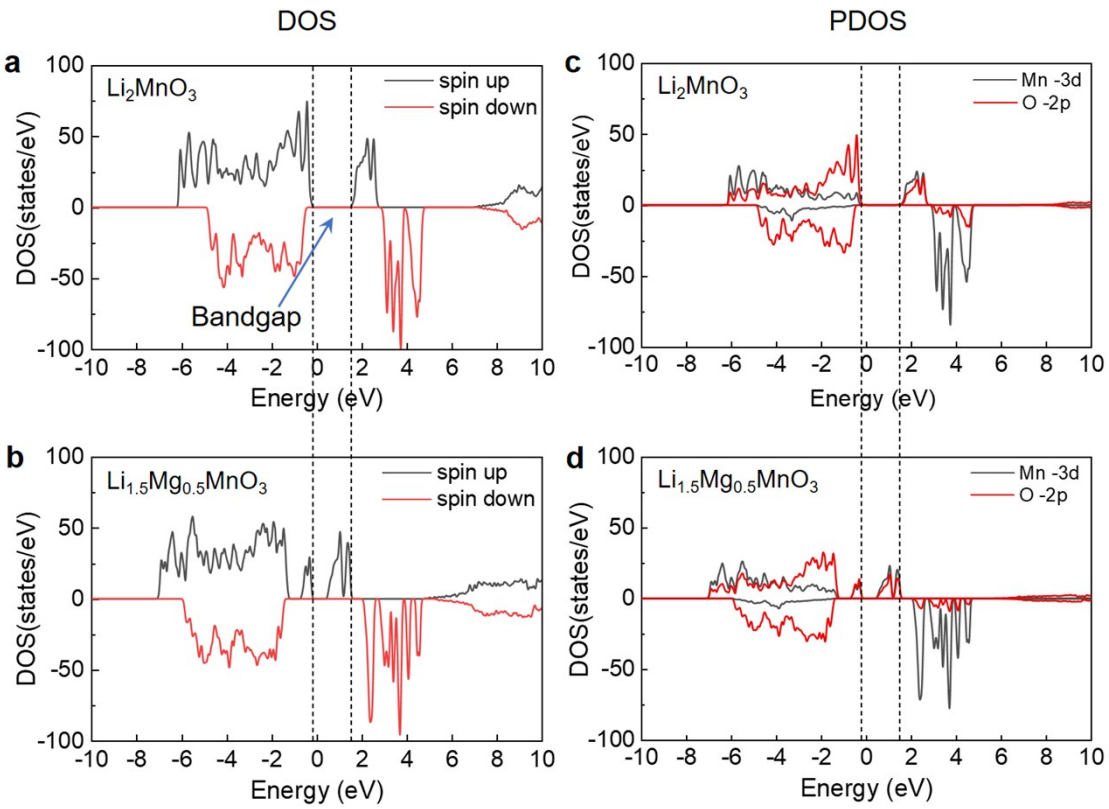

Figure S5. The TDOS and pDOS of LMO and LMMO are based on spin-up and spin-down, and the pDOS is based on 3*d* orbitals of TM atoms and 2*p* orbitals of O atoms.

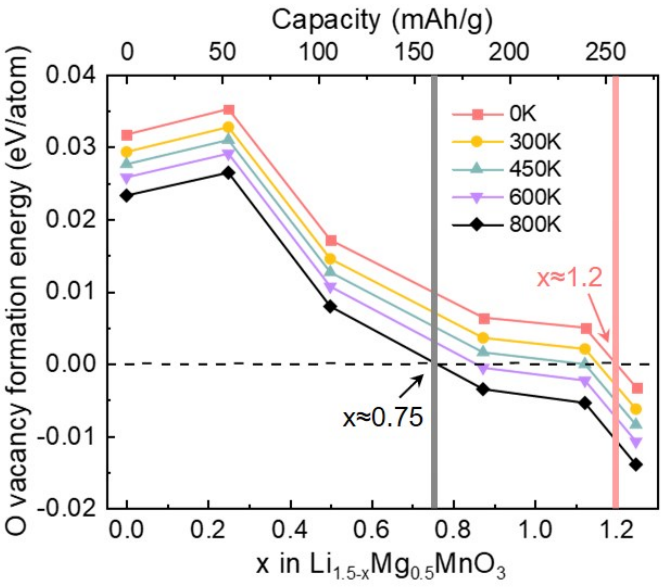

Figure S6. Formation energy of oxygen vacancy during delithiation at 0 K, 300 K, 450 K, 600K and 800 K respectively.

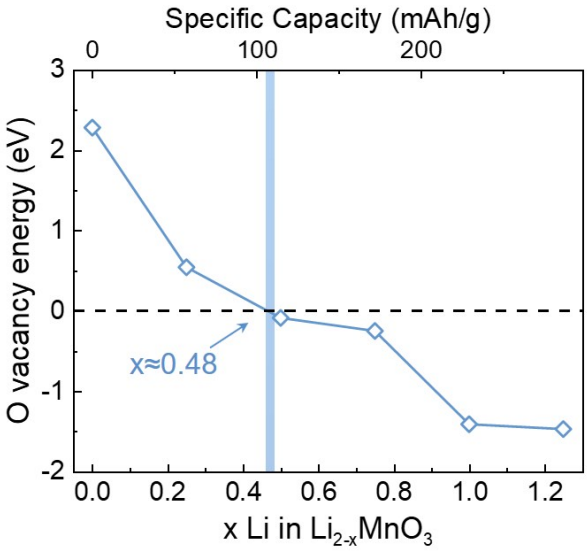

Figure S7. The reversible and irreversible regions in Li_2MnO_3 are based on thermodynamics: oxygen vacancy formation energy (blue solid line) at $\Delta E\_vac=0$ (black dashed line), $x \approx 0.48$ is the boundary between the reversible and irreversible regions.

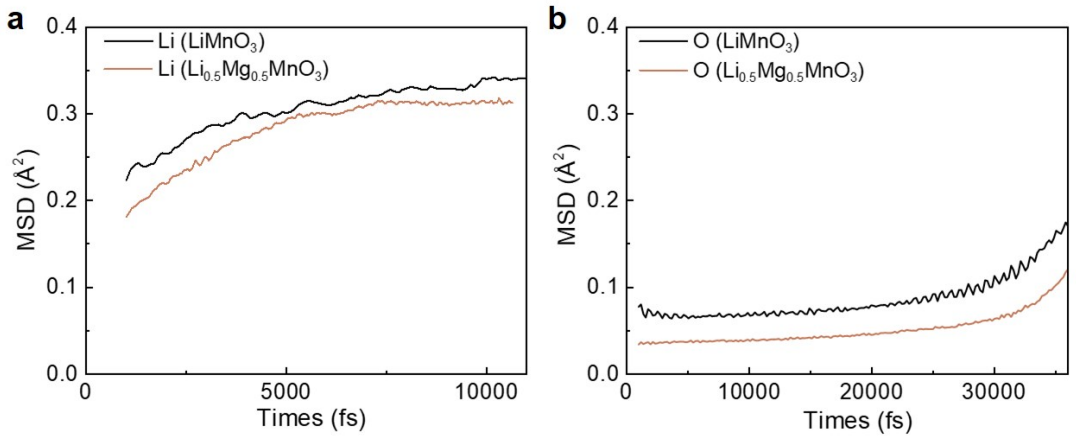

Figure S8. The Mean Square Displacement of Li and O in $LiMnO_3$ and $Li_{0.5}Mg_{0.5}MnO_3$ in (T=300K).

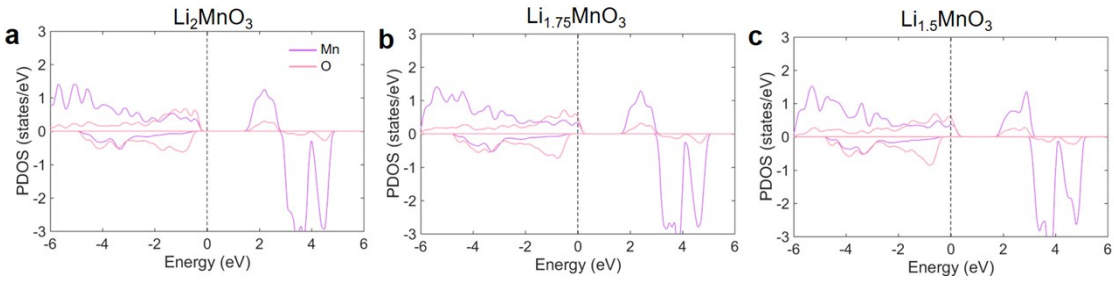

Figure S9. The pDOS of $Li_{2-x}MnO_3$ (x=0, 0.25, 0.5).

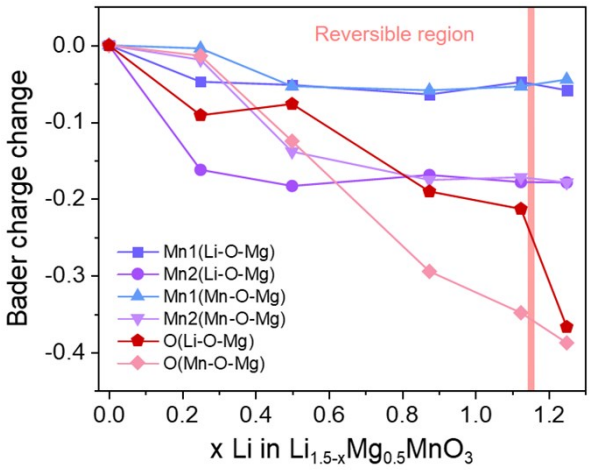

Figure S10. The Bader charge changes of oxygen and Mn ions during the delithiation.

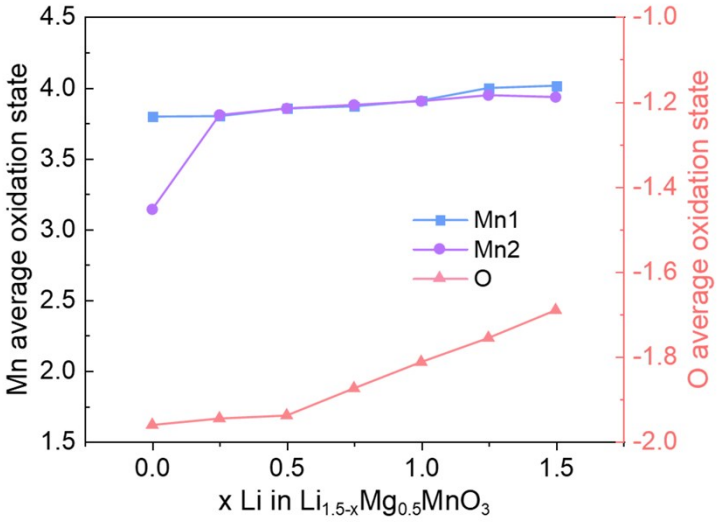

Figure S11. The calculated average oxidation state of Mn and O atoms as a function of delithiation (x in $Li_{1.5-x}Mg_{0.5}MnO_3$). Two Mn-ions with linear and perpendicular distributions of 2(Mn-O-Mg) present different charge states of +3.8 (Mn1) and +3.15 (Mn2), respectively.